Thermal conductivities of individual tin dioxide nanobelts

Li Shi,[a] Qing Hao, and Choongho Yu
Department of Mechanical Engineering and Center for Nano and Molecular Science and Technology, Texas Materials Institute, The University of Texas at Austin, Austin, Texas 78712

Natalio Mingo
Eloret Corporation, NASA-Ames Research Center, Moffet Field, California 94035

Xiangyang Kong and Z. L. Wang
School of Materials Science and Engineering, Georgia Institute of Technology, Atlanta, Georgia 30332

(Received 18 November 2003; accepted 12 February 2004)

We have measured the thermal conductivities of a 53-nm-thick and a 64-nm-thick tin dioxide (SnO_2) nanobelt using a microfabricated device in the temperature range of 80–350 K. The thermal conductivities of the nanobelts were found to be significantly lower than the bulk values, and agree with our calculation results using a full dispersion transmission function approach. Comparison between measurements and calculation suggests that phonon–boundary scattering is the primary effect determining the thermal conductivities. © *2004 American Institute of Physics.*
[DOI: 10.1063/1.1697622]

Ribbon or beltlike nanostructures of metal oxides have recently been synthesized using a vapor–solid method.[1,2] These nanobelts of tin dioxide (SnO_2), zinc oxide (ZnO), indium oxide (In_2O_3), and gallium oxide (Ga_2O_3) have a rectangular cross section with a thickness of 10–100 nm and a width of 50–500 nm. Distinguished from carbon nanotubes and other semiconductor nanowires, the metal–oxide nanobelts are single-crystalline semiconductors without the presence of a surface insulating layer of native oxides. These properties make nanobelts attractive for applications in transparent electronics and nanosensors. As of today, field effect transistors,[3] ultrasensitive gas sensors,[4] and nanocantilevers[5] have been fabricated using SnO_2 or ZO nanobelts.

Additionally, these metal–oxide nanobelts provide a unique system for studying phonon transport in low-dimension materials. Recently, superhigh and significantly suppressed thermal conductivities were observed in carbon nanotubes and semiconductor nanowires, respectively.[6–8] The two opposite results are attributed to the unique crystalline structure of carbon nanotubes and an increased phonon–boundary scattering rate in nanowires,[9] while other phonon confinement effects in nanowires have also been suggested.[10] These nanoscale thermal transport properties can impact the performance and reliability of nanoelectronics,[11] and may find potential use for improving the thermoelectric figure of merit of Peltier devices.[12,13] Compared to the knowledge obtained for nanotubes and nanowires, little has been known regarding the thermal properties of metal–oxide nanobelts, which have a distinctively different structure and many promising applications.

We have measured the thermal conductivities of a 53-nm-thick, 204-nm-wide, and a 64-nm-thick, 108-nm-wide SnO_2 nanobelt in the temperature range of 80–350 K. We have observed that the thermal conductivities of the nanobelts were strongly suppressed compared to the bulk values. According to our calculation using a full dispersion transmission function approach, moreover, it appears that the suppressed thermal conductivities can be attributed mainly to an increased phonon–boundary scattering rate although other confinement effects might still play a role.

We used a microfabricated device for the thermal measurement. Details on the measurement method can be found elsewhere.[14] In brief, the microdevice was a suspended membrane structure consisting of two suspended SiN_x membranes, as shown in Fig. 1. A platinum (Pt) serpentine is patterned on each membrane, serving as a heater and resistance thermometer (RT). A separate Pt electrode is patterned on the edge of each membrane. The SnO_2 nanobelt was deposited on a Pt electrode pair using a wet deposition method. In this method, a collection of SnO_2 nanobelts was dissolved in isopropanol or ethanol in an ultrasonic bath. A drop of the solution was then deposited on a diced wafer containing about twenty microdevices. The solution was subsequently spun off the wafer. This procedure often yielded SnO_2 nanobelts trapped on a Pt electrode pair and bridging the two suspended SiN_x membranes. The inset of Fig. 1 shows a

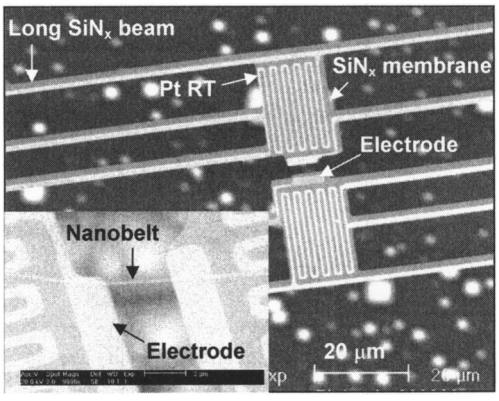

FIG. 1. A microfabricated device for measuring the thermal conductivity of a nanostructure. Inset: A 53-nm-thick SnO_2 nanobelt trapped on the two Pt electrodes of the device.

[a]Author to whom correspondence should be addressed; electronic mail: lishi@mail.utexas.edu

53-nm-thick SnO_2 nanobelt bridging the two membranes. The suspended segment of the nanobelt between the two membranes was 3.16 μm long. Each of the two segments deposited on the two membranes was more than 6 μm long.

During the measurement, the sample was kept in an evacuated continuous flow liquid-helium cryostat. A dc current (I) was supplied to one Pt serpentine to raise the temperature of the membrane supporting the serpentine. Part of the Joule heat generated in the heating membrane was conducted through the SnO_2 nanobelt to the other membrane (the sensing membrane). The temperature rises in the two membranes were measured using the two Pt RTs by measuring its differential electrical resistance (R_h). The thermal conductance (G_s) of the nanobelt is obtained as

$$G_s = \frac{Q_h + Q_L}{\Delta T_h + \Delta T_s} \frac{\Delta T_s}{\Delta T_h - \Delta T_s}, \tag{1}$$

where $Q_h = I^2 R_h$ is the Joule heating in the heating Pt serpentine, Q_L is the Joule heating in one of the two Pt leads supplying the dc current (I) to the heating serpentine, and ΔT_h and ΔT_s are the temperature rise in the heating and sensing membranes, respectively. During the experiment, we increased ΔT_h up to 2 K by ramping up the dc current (I). The small temperature excursion allows one to assume that G_b and G_s were constant as ΔT_h was ramped up.

The measurement errors due to radiation and heat conduction through the residual gas in the evacuated cryostat are estimated to be negligible. The major measurement error is the contact thermal conductance (G_c) between the nanobelt and the membrane, because the measurement result consists of a contribution from G_c as well as the intrinsic thermal conductance of the nanobelt (G_n), i.e.,

$$G_s = (G_n^{-1} + G_c^{-1})^{-1}. \tag{2}$$

One can estimate that $G_c \approx 2\pi(\kappa_n^{-1} + \kappa_m^{-1})^{-1} a$, where κ_n and κ_m are the thermal conductivity of the nanobelt and membrane, respectively, and a is the contact spot size between the nanobelt and the membrane. For a very small contact spot $a \sim 10$ nm, we estimated that G_c was at least one order of magnitude larger than the measured G_s of the two nanobelts. Since the two nanobelts were more than 100 nm wide and each of their two segments deposited on the two membranes was more than 3 μm long, the contact spot size is expected to be much larger than 10 nm. To further confirm $G_c \gg G_s$, we have also measured a 232-nm-thick and a 178-nm-thick nanobelt, for which G_n was expected to be closer to G_c than for the two much thinner samples. The G_s of the two thick nanobelts were found to be more than ten times larger than those of the two thinner samples. As all four samples have a similar contact area with the membranes, G_c should not vary significantly from the thick to the thin samples. Hence, as G_c is always larger than G_s for the thick nanobelts, G_c should be at least ten times larger than the G_s of the thin ones. Therefore, we concluded that for the two thin samples, $G_c \gg G_s$ and $G_s = G_n$ to all effects.

The thickness (t) of the nanobelt was measured using a tapping mode atomic force microscope to map the segment of the nanobelt laid on one membrane; while the length (L) and width (w) of the nanobelt were obtained using a high-resolution scanning electron microscope. The thermal conductivities of the nanobelts were calculated according to $\kappa_n = G_s L/wt$, and plotted in Fig. 2. The obtained thermal conductivities were found to be substantially lower than the bulk values.[15]

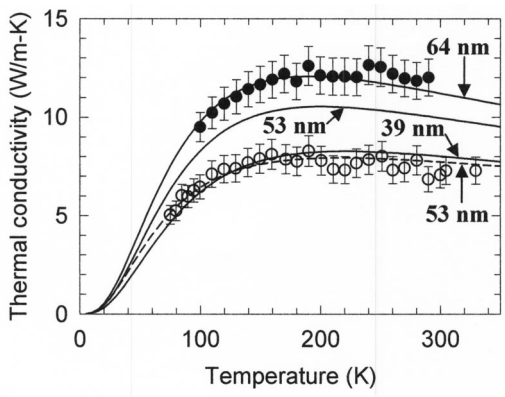

FIG. 2. Thermal conductivities of a 64-nm-thick (solid circles) and a 53-nm-thick (open circles) SnO_2 nanobelt as a function of temperature. Also shown are calculation results (lines) with the bulk parameters for the Umklapp process and different FL values indicated for each line. An impurity scattering rate ten times of the bulk value is used for the dashed line; while the bulk value is used for the three solid lines.

To understand the origins of the reduced thermal conductivities, we have used a full dispersion transmission function approach for thermal calculation. The calculation procedure will be reported in a separate paper and a detailed description of the method can be found elsewhere.[16,17] In the calculation, we obtained the nanobelt dispersion relations for the rutile structure. Matthiessen's rule was used to obtain the frequency-dependent relaxation time of phonons as $\tau^{-1} = \tau_U^{-1} + \tau_b^{-1} + \tau_i^{-1}$.[18] Here, τ_U^{-1}, τ_b^{-1}, and τ_i^{-1} are the Umklapp, boundary, and impurity scattering rates, respectively. A phenomenological expression for the Umklapp scattering rate has been used: $\tau_U^{-1} = Be^{-b/T}\omega^2 T$, where B and b are two fitting parameters. The boundary and impurity scattering rates can be written as $\tau_b^{-1} = \nu/FL$ and $\tau_i^{-1} = A\omega^4$. Here, L is the characteristic length of the system (thickness for the nanobelt samples), F is a parameter representing specularity of phonon reflection at the boundaries, the FL product is referred as the effective thickness of the sample, and A is a parameter arising from Rayleigh scattering of phonons by atomic scale impurities.

In determining the parameters for $\tau(\omega)$, measurements of the bulk SnO_2 thermal conductivity in the (100) or $C_\perp$ direction and the (001) or $C_\parallel$ direction were used.[15] Because we could not find bulk measurement data for the (101) direction, the usual growth direction of the SnO_2 nanobelts, we estimated the bulk values for this direction by considering the (100) and (001) values to be the components of the diagonal conductivity tensor.

After obtaining the fitting parameters from the bulk measurement data, we calculated the thermal conductivities of nanowires by varying the effective thickness FL while keeping other parameters as the same as the bulk values. The solid lines of Fig. 2 are three sets of calculated thermal conductivities in the (101) direction as a function of temperatures. One can see that the measurement data of the 64-nm-thick and 53-nm-thick SnO_2 nanobelt agree rather well with the calculation results with $FL = 64$ nm and 39 nm, respec-

tively. This suggests that an increased phonon–boundary rate alone can well account for the significantly suppressed thermal conductivities of the nanobelts,[19] although other effects cannot be ruled out completely. For example, we found that the measurement results of the 53 nm sample can also be fitted with the bulk Umklapp parameters, a *FL* value of 53 nm, and an impurity scattering rate ten times higher than the bulk value, as shown as the dashed line in Fig. 2. The difference in surface specularity or impurity scattering rate between the two samples can be due to different surface roughness or impurity concentrations.

In summary, we have measured the thermal conductivities of SnO_2 nanobelts, another class of nanostructures with a distinct structure and many promising applications. The observed thermal conductivities are significantly lower than the bulk values, and are attributed to an increased phonon–boundary scattering rate, although the influence of other effects, such as increased impurity scattering, cannot be ruled out.

This work is supported by a CAREER award and an instrumentation grant to one of the authors (L.S.) by the Chemical and Transport Division of the National Science Foundation. The authors thank D. Li and A. Majumdar for helpful discussions.

[1] Z. Pan, Z. Dai, and Z. L. Wang, Science **291**, 1947 (2001).
[2] Z. R. Dai, Z. W. Pan, and Z. L. Wang, Adv. Functional Materials **13**, 9 (2003).
[3] M. Arnold, P. Avouris, Z. W. Pan, and Z. L. Wang, J. Phys. Chem. B **107**, 659 (2002).
[4] E. Comini, G. Faglia, G. Sberveglieri, Z. W. Pan, and Z. L. Wang, Appl. Phys. Lett. **81**, 1869 (2002).
[5] W. Hughes and Z. L. Wang, Appl. Phys. Lett. **82**, 2886 (2003).
[6] P. Kim, L. Shi, A. Majumdar, and P. L. McEuen, Phys. Rev. Lett. **87**, 215502 (2001).
[7] D. Li, Y. Wu, P. Kim, L. Shi, P. Yang, and A. Majumdar, Appl. Phys. Lett. **83**, 2934 (2003).
[8] D. Li, Y. Wu, R. Fan, P. Yang, and A. Majumdar, Appl. Phys. Lett. **83**, 3186 (2003).
[9] S. G. Volz and G. Chen, Appl. Phys. Lett. **75**, 2056 (1999).
[10] J. Zhou and A. Balandin, J. Appl. Phys. **89**, 2932 (2001).
[11] P. G. Sverdrup, Y. S. Ju, and K. E. Goodson, J. Heat Transfer **123**, 130 (2001).
[12] Y.-M. Lin, X. Sun, and M. S. Dresselhaus, Phys. Rev. B **62**, 4610 (2000).
[13] G. Chen and A. Shakouri, J. Heat Transfer **124**, 242 (2002).
[14] L. Shi, D. Li, C. Yu, W. Jang, D. Kim, Z. Yao, P. Kim, and A. Majumdar, J. Heat Transfer **125**, 881 (2003).
[15] P. Türkes, C. Pluntke, and R. Helbig, J. Phys. C **13**, 4941 (1980).
[16] N. Mingo, Phys. Rev. B **68**, 113308 (2003).
[17] N. Mingo, L. Yang, D. Li, and A. Majumdar, Nano Lett. **3**, 1713 (2003).
[18] J. E. Parrot and A. D. Stuckes, *Thermal Conductivity of Solids* (Pion, London, 1975).
[19] For an isotropic material with a rectangular cross section, an *F* value in the range of 1.4–2 would be expected for totally diffusive boundary scattering. Nevertheless, the fact that the rutile structure of SnO_2 is very anisotropic, with higher speeds of sound in the directions perpendicular to the growth axis, can result in lower values of *F*, close to 1 in the present case.